



Progress in triacylglycerol isomer detection in milk lipids

Huiru Cao^{a,b,c,1}, Qian Liu^{a,b,c,1}, Yan Liu (刘妍)^{b,c,1}, Junying Zhao^{b,c}, Weicang Qiao^{b,c}, Yuru Wang^{a,b,c}, Yan Liu (刘言)^{b,c}, Lijun Chen^{a,b,c,*}

^a Key Laboratory of Dairy Science, Ministry of Education, Food Science College, Northeast Agricultural University, Harbin 150030, China

^b National Engineering Research Center of Dairy Health for Maternal and Child, Beijing Sanyuan Foods Co. Ltd., Beijing 100163, China

^c Beijing Engineering Research Center of Dairy, Beijing Technical Innovation Center of Human Milk Research, Beijing Sanyuan Foods Co. Ltd., Beijing 100163, China

ARTICLE INFO

Keywords:

Triacylglycerol
Isomers
Chromatogram
Ion fragment

ABSTRACT

In triacylglycerols (TAGs), position differences of fatty acids on the glycerol skeleton produce various TAG isomers. These TAG isomers have different pathways of digestion, absorption, and utilization in infants, thereby affecting TAG nutritional properties of TAGs. Here, we review the progress of research on methods for detecting TAG isomers, and identify direction and thought for improving these methods, including novel chromatographic combinations, perfect algorithm, and improved equipment. The ensuing optimization of these methods is expected to provide robust guarantee for the gradual improvement of milk-derived TAG isomer detection, and is an important prerequisite for infant formula to mimic the structured lipids of human milk.

1. Introduction

Human milk is the optimum food for infants, especially those in their first six months of life (Chen et al., 2019). The lipids in human milk provide approximately 50% of the energy required by infants (Bourliou et al., 2015), promote the development of the infant central nervous system (Dean et al., 2014), improve immunity, and control inflammation (Jakaitis & Denning, 2014). Triacylglycerols (TAGs) account for >98% of human milk lipids (Zhao et al., 2021).

TAGs are mainly formed through the esterification of one molecule of glycerol and three molecules of fatty acids (FAs) (Liu, Rochfort, & Cocks, 2018). The position of FAs on the glycerol backbone is described according to the stereospecific numbering (*sn*) system as the *sn*-1, *sn*-2, and *sn*-3 positions (Wei et al., 2020). In addition to classifying TAG molecules according to their different fatty acyls, their isomers can be categorized into three types: TAG isomers (same molecular weight but different fatty acyls), such as TAG 50:2, *sn*-16:0-16:0-18:2 and TAG

50:2; *sn*-16:0-16:1-18:1; TAG regioisomers (same fatty acyls but different positional distribution), such as *sn*-16:0-18:1-16:0 and *sn*-16:0-16:0-18:1; and TAG enantiomers (different structure in the Fischer projection), such as *sn*-16:0-16:0-18:1 and *sn*-18:1-16:0-16:0. If three different FAs are represented by A, B, and C, the above three isomers can be represented as shown in Fig. 1, where a, b, and c have the same total molecular weight as A, B, and C, and *rac*-ABC denotes the racemic mixture of *sn*-ABC and *sn*-CBA (Yoshinaga, 2021).

Approximately 70% or more of the palmitic acid (P) in human milk is located at the *sn*-2 position of TAGs, while unsaturated fatty acids (UFAs), especially oleic acid (O) and linoleic acid (L), are located at the *sn*-1 and *sn*-3 positions (Sun, Wei, Su, Zou, & Wang, 2018). The most abundant TAGs are 1,3-dioleoyl-2-palmitoylglycerol (OPO) and 1-oleoyl-2-palmitoyl-3-linoleoylglycerol (OPL), belonging to *sn*-2 palmitate TAGs, which promote the absorption of calcium and other minerals by infants, softens their stool, and reduces crying (Miles & Calder, 2017). In human milk, the TAG species and isomers play important

Abbreviations: APCI-MS, atmospheric pressure chemical ionization-mass spectrometry; CID, collision-induced dissociation; DAG, diacylglycerol; EAD, electron-activated dissociation; ECD, electron capture dissociation; EIEIO, electron impact excitation of ions from organic compounds; ESI, electrospray ionization; FA, fatty acid; La, lauric acid; L, linoleic acid; LC-MS, liquid chromatography-mass spectrometry; LC-PUFA, long-chain polyunsaturated fatty acid; LC-UFA, long-chain unsaturated fatty acid; MS, mass spectrometry; MAG, monoacylglycerol; NMR, nuclear magnetic resonance; O, oleic acid; P, palmitic acid; Po, palmtoleic acid; PPL, porcine pancreatic lipase; PFL, *Pseudomonas fluorescens* lipase; SFA, saturated fatty acid; Ag-HPLC, silver ion high-performance liquid chromatography; S, stearic acid; SFC, supercritical fluid chromatography; St, stearyl; TAG, triacylglycerol; UHPLC, ultra-high-performance liquid chromatography; UPSFC-Q-TOF-MS, ultra-performance SFC and quadrupole time-of-flight mass spectrometry; UFA, unsaturated fatty acid.

* Corresponding author at: Beijing Sanyuan Foods Co., Ltd., No. 8, Yingchang Street 100076, Yinghai Town, Daxing District, Beijing, China.

E-mail address: chenlijun@sanyuan.com.cn (L. Chen).

¹ These authors contributed equally.

<https://doi.org/10.1016/j.fochx.2024.101433>

Received 1 February 2024; Received in revised form 26 April 2024; Accepted 29 April 2024

Available online 3 May 2024

2590-1575/© 2024 Published by Elsevier Ltd. This is an open access article under the CC BY-NC-ND license (<http://creativecommons.org/licenses/by-nc-nd/4.0/>).

nutritional and physiological roles; therefore, the detection of TAG isomers and understanding of their structure and distribution are essential for the design of infant formulas that provide nutritional values similar to those of human milk.

Although numerous studies have focused on the function of TAG isomers and the development of their detection methods, few of them systematically analyze and compare these detection methods. Systematically analysis the current status of structured TAG isomer detection methods, identifying the advantages and disadvantages of existing methods as well as their correlation and differences, and seeking new combinations and innovations are the icebreaker to solve the bottleneck of structured TAGs isomer detection. In this paper, we summarize the functions of TAG isomers and the advantages and disadvantages of different methods for TAG isomer detection. Subsequently, ideas are proposed for improving TAG isomer detection to facilitate the identification and simulation of the structural lipids in human milk. A comprehensive isomer analysis method is the guarantee for clarifying the characteristics of structured TAGs from milk-derived, meanwhile it is also the necessary pathway to shorten the gap between infant formula and human milk in structured TAGs.

2. Applications of specifically structured TAG isomers in infant food

Approximately 80% of OOP in human milk has the *sn*-OPO structure, and a very small fraction has the *sn*-OOP structure (Zhang, Wei, Tao, Jin, & Wang, 2021). The position of FAs in the glycerol skeleton can affect the metabolism of TAGs, which may affect infant health. Non-*sn*-2 palmitate TAGs (such as *sn*-OOP) are hydrolyzed in the intestine produce free long-chain unsaturated fatty acids (LC-UFAs), palmitic acid, and *sn*-2 unsaturated fatty acyl monoacylglycerols (MAGs). *Sn*-2 MAGs and free LC-UFAs are directly absorbed by the epithelial cells of the small intestine (Hageman, Danielsen, Nieuwenhuizen, Feitsma, & Dalsgaard, 2019). Palmitic acid reacts easily with Ca^{2+} to form calcium soap that cannot be absorbed by the intestines, which not only results in the loss of calcium and FAs but also hampers bowel movements in infants (Béghin et al., 2019). In contrast, *sn*-2 palmitate TAGs (such as *sn*-OPO) are hydrolyzed in the intestine into two free LC-UFAs and *sn*-2

palmitate MAG, which are directly absorbed by the small intestine and do not easily generate calcium soap with Ca^{2+} . This can effectively reduce constipation in infants, improve the utilization of FAs, increase calcium absorption, and promote bone development (Fig. 2) (Litmanovitz et al., 2013; Manios et al., 2020; Zhu et al., 2023).

The *sn*-2 palmitate TAGs also affect infant gut flora in terms of microbial diversity, abundance, and composition. *Actinomycetes*, *Proteobacteria*, *Firmicutes*, and *Bacteroides* are known to be abundant in the feces of toddlers (Hou, Xiao, & Li, 2019). A previous study showed that the amounts of *Bacteroides* and *Firmicutes* significantly correlated with content of TAGs with palmitic acid at the *sn*-2 position, and the correlation between *Firmicutes* and palmitic acid at the *sn*-2 position increases with the increase in breastfeeding time (Jiang et al., 2018). The *sn*-2 palmitate TAGs also help to increase the abundance of *Bifidobacterium* (Fig. 2) (Chen et al., 2022; Wang et al., 2023). A recent study analyzed the impact of infant formulas containing *sn*-2 palmitate TAGs on the fecal microflora and metabolomic characteristics of healthy full-term infants (Guo et al., 2022). At week eight, the abundance of intestinal *Bifidobacterium* and intestinal microbiota α -diversity increased and the abundance of *Escherichia-Shigella* decreased in the group fed with *sn*-2 palmitate TAG formula compared to those in infants fed a regular plant-based formula. Another study showed that increasing the abundance of intestinal *Bifidobacterium* using *sn*-2 palmitate TAG has a favorable effect on infant neurodevelopment, thereby promoting the development of fine motor skills in infants (Wu et al., 2021).

3. Detection of TAG isomers

3.1. Enzymatic hydrolysis method

Enzymatic hydrolysis has been widely adopted to determine TAG isomers for several decades. Lipase is a serine hydrolase that hydrolyzes the ester bond of TAG to produce diacylglycerols (DAG), MAG, glycerol, and FA (Choi, Park, & Chang, 2021) and has unique catalytic activities for a wide range of substrates during hydrolysis, acidolysis, alcoholysis, and esterification, for which the regioselectivity and stereoselectivity are important properties (Abdi Hasibuan, Sitanggang, Andarwulan, & Hariyadi, 2021). Regioselectivity refers to the ability of lipase to

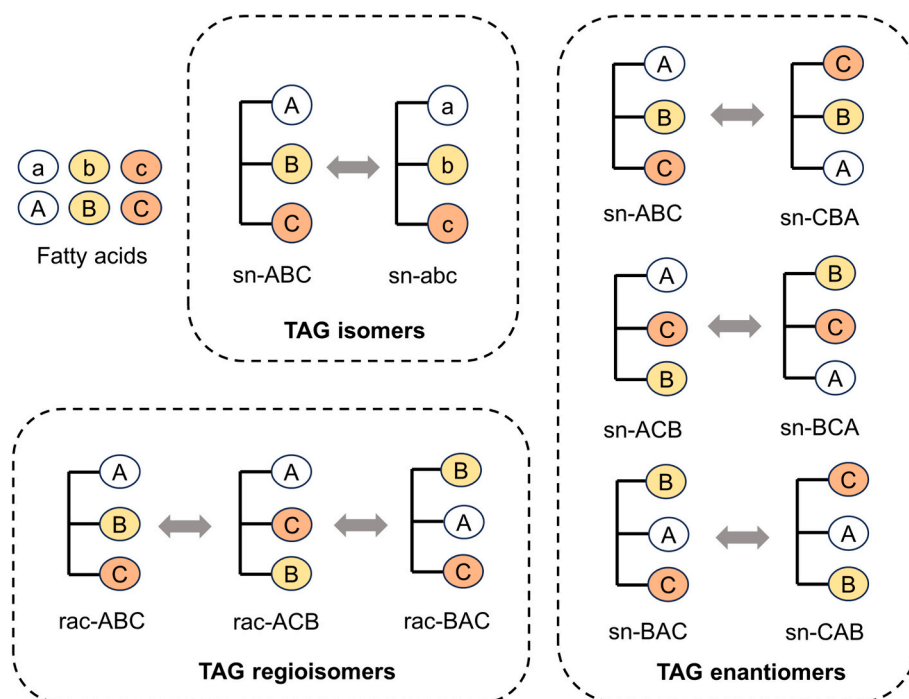


Fig. 1. Structural schematic diagram of TAG isomers, regioisomers, and enantiomers.

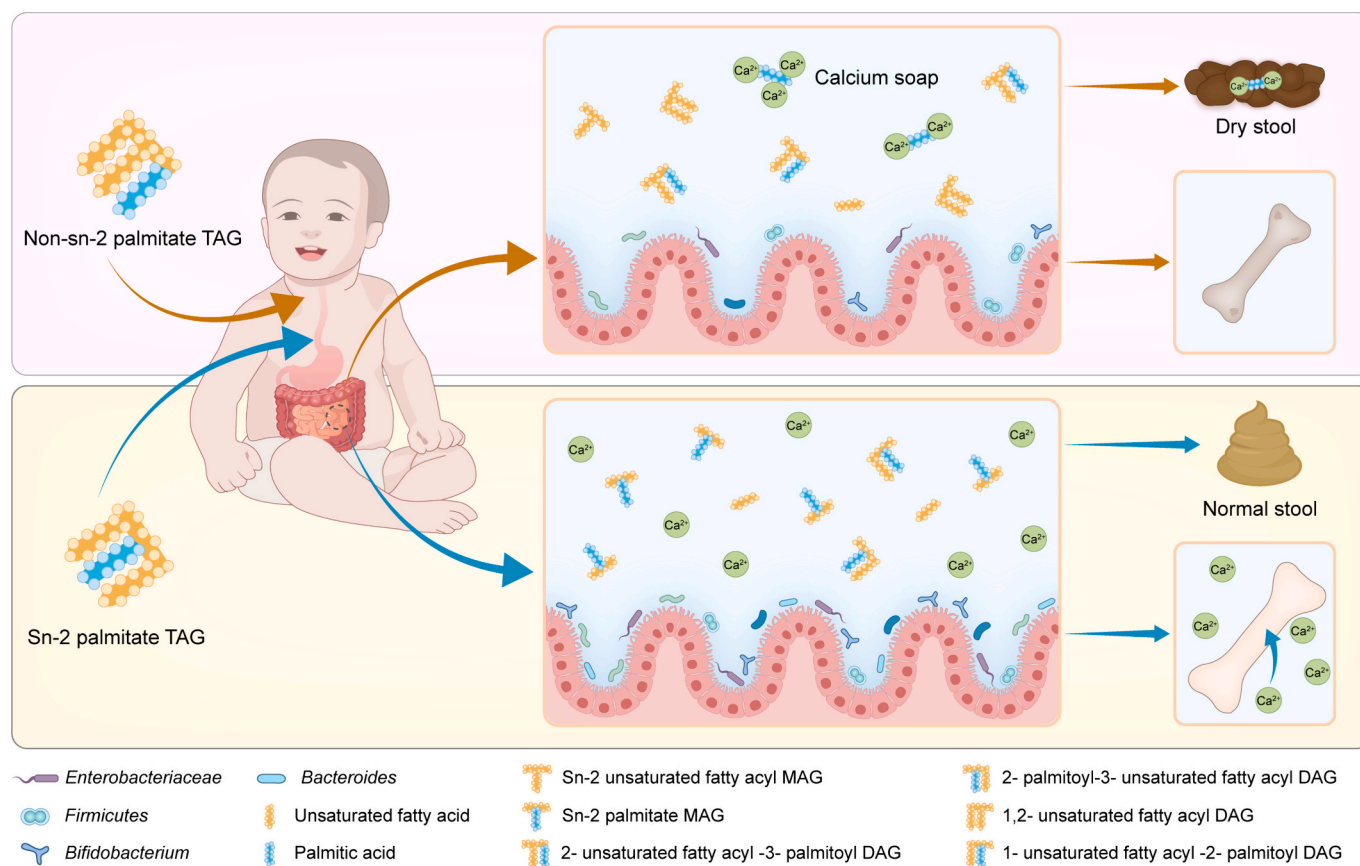


Fig. 2. Effects of TAG isomers on intestinal health and bone development of infants.

recognize and hydrolyze the ester bond at *sn*-1 or *sn*-3 rather than that at *sn*-2, whereas the stereoselectivity refers to the ability to recognize and hydrolyze the ester bond at *sn*-1 or *sn*-3 in a stereospecific structure (Choi & Chang, 2022). The regioselectivity of lipases is particularly important for the lipase-catalyzed catabolism of TAGs. Most lipases are regioselective for the *sn*-1 and *sn*-3 positions of TAGs and are therefore called *sn*-1,3-specific lipases, including pancreatic, pre-gastric, and microbial lipases (Wei et al., 2020). Only a few lipases are known to possess *sn*-3 regioselectivity (e.g., gastric lipase (Roman et al., 2007) and rabbit gastric lipase (Yuan et al., 2020)) or *sn*-2 regioselectivity (*Candida antarctica* A lipase (Monteiro et al., 2021)). A study on the digestion of DAG isomers by gastric lipase showed that the activity of gastric lipase on *sn*-1,3-DAG was greater than that on *sn*-1,2-DAG, *sn*-2,3-DAG, and TAG (Bakala-N'Goma et al., 2022). Another study showed that *Pseudomonas fluorescens* lipase (PFL) is selective for the *sn*-1 position of TAGs, especially for long-chain polyunsaturated fatty acids (LC-PUFAs) but shows no stereoselectivity for *sn*-1,3-DAGs. In contrast, porcine pancreatic lipase (PPL) exhibits no difference in regional selectivity between the *sn*-1 and *sn*-3 positions of TAG but does show stereoselectivity for the *sn*-1 position of *sn*-1,3-DAGs (Kozlov et al., 2023).

Pancreatic lipase is a *sn*-1,3-specific lipase that is commonly used to hydrolyze TAGs. It is mainly combined with gas chromatography to detect the FA distribution at *sn*-2 in TAGs. PPL from Sigma-Aldrich is the most widely used product, and, to date, PPL has been used to hydrolyze TAGs in colostrum and mature human milk to analyze the distribution of FAs (Deng et al., 2018). Free FAs and *sn*-2 MAGs were then methylated and detected using gas chromatography. Another research team adopted the same method to analyze the FA composition and *sn*-2 position distribution of TAGs in human milk during different lactation periods (Qi et al., 2018). Unfortunately, enzymatic hydrolysis only provides the distribution of FAs at the *sn*-1,3 and *sn*-2 positions of TAGs, and it cannot

be used to obtain structural information related to single TAG regioisomers. To obtain detailed structural information about single TAG regioisomers, other analytical techniques are required.

3.2. Gas chromatography–mass spectrometry methods

Owing to its versatility and cost effectiveness, gas chromatography (GC) using high temperature and medium polarity columns is utilized as a routine analytical method. Typically, the GC is equipped with a TAG-specific neutral polarity column and utilizes gas pressure gradient to separate TAG substances for initial separation. This system is effective in separating the TAGs in common vegetable oils and fats (e.g., sunflower oil, shea butter, and cocoa butter) (Salas, Bootello, Martínez-Force, & Garcés, 2011). When coupled with MS, this method can provide structural information about TAGs. Recently, a GC–MS method was developed to isolate unsaturated TAGs (*sn*-POP/*sn*-PPO, *sn*-PLP/*sn*-PPL, *sn*-POST/*sn*-PStO/*sn*-StPO, *sn*-StOSt/*sn*-StStO (where St is stearoyl)) directly from vegetable oils and fats, and the structural information of TAG regioisomers was derived from the mass spectrometry data (Garcés, Martínez-Force, Venegas-Calderón, Moreno-Pérez, & Salas, 2023). The TAG regioisomers are identified based on the varying intensities of the resulting FA fragmentation signals and can be consistently quantified by selected ion monitoring integration. This approach is popular in plant lipid analysis, which might be a good option for improving the analysis of milk lipid regioisomers.

3.3. Liquid chromatography–mass spectrometry methods

Liquid chromatography–mass spectrometry (LC-MS) technologies based on silver ion high-performance liquid chromatography (Ag-HPLC), chiral chromatography, and ultra-high-performance liquid chromatography (UHPLC) have been recently developed to analyze TAG

isomers (Fabritius et al., 2020). The liquid chromatographic separation resolution depends on factors such as the type of chromatographic column, column temperature, column flow rate, and injection volume (Li et al., 2018), whereas mass spectrometry (MS) detection is affected by factors such as the ion source temperature, capillary temperature, collision energy, and scanning range. Table 1 lists the detection results of TAG isomers under different LC-MS conditions.

3.3.1. Chromatographic columns

3.3.1.1. Silver ion chromatographic columns. Ag-HPLC separates TAG regioisomers according to the saturation and position of double bonds in the FAs, and retention is based on the ability of unsaturated organic compounds to form complexes with transition metals on the stationary phase. In the formed charge-transfer-type organometallic complexes, the unsaturated compounds serve as the electron donor and silver ions serve as the electron acceptor. TAGs with different numbers and positions of double bonds can be isolated according to the strength of weakly reversible complexes that form during elution (Arena, Sciarrone, Dugo, & Mondello, 2021). Currently, almost all Ag-HPLC-MS systems use Ag⁺ columns based on ion exchangers. In these exchangers, Ag⁺ ions replace protons in the sulfonic acid functional group, and the resultant silver sulfonate ions interact with C=C double bonds during chromatographic analysis. The ionic bond between sulfur and silver is quite stable, and thus, no Ag⁺ leakage occurs, even after prolonged use in HPLC (Holapek & Lřsa, 2017).

Using a Luna SCX Ag⁺ chromatographic column coupled with atmospheric pressure chemical ionization–mass spectrometry (APCI-MS), (Santoro et al., 2018) performed gradient elution with *n*-heptane and ethylacetate (93:7 and 90:10 v/v) as the mobile phase. They successfully isolated and characterized three pairs of TAG regioisomers consisting of stearic acid (S), palmitic acid, and oleic acid (*sn*-POP/*sn*-PPO, *sn*-POS/*sn*-PSO, and *sn*-POO/*sn*-OPO). In a different study, a ChromSpher lipids column using heptane as the mobile phase was coupled to APCI-MS to investigate the effect of column temperature (5–35 °C) on the retention time and separation of five pairs of regioisomers (*sn*-SOS/*sn*-SSO, *sn*-POS/*sn*-PSO, *sn*-POP/*sn*-PPO, *sn*-SOO/*sn*-OSO, and *sn*-POO/*sn*-OPO) (Gorska et al., 2023). The results showed that the retention time and resolution of the TAG isomers increased with the increase in column temperature, but it also increased the peak width and decreased the peak intensity. These studies demonstrate the importance of optimizing chromatographic conditions (e.g., mobile phase composition and column temperature) to achieve optimal separation and characterization of the recombinant regioisomers of TAG. Moreover, the use of the relatively less toxic heptane as the mobile phase in both experiments is indicative of the desire for relatively safe reagents in lipid research. Owing to the complex composition of human milk TAGs, C18 columns are primarily used to separate the target TAG before conducting Ag-HPLC analysis (Chen et al., 2019; Chen, Zhou, Han, Yu, & Zhang, 2020). Although Ag-HPLC has obvious advantages for the separation of TAG isomers (i.e., high-resolution), commercial Ag-HPLC columns are expensive, whereas self-made columns are complicated to prepare, and their service life is short (usually several months). Meanwhile, Ag⁺ columns must be regenerated periodically, which may also cause problems, including poor reliability and repeatability (Momchilova & Nikolova-Damyanova, 2022).

3.3.1.2. Chiral chromatographic columns. Chiral stationary-phase chromatography is an efficient, selective, and widely used technique for chiral separation. The chiral recognition is based on the formation of diastereomer complexes with different stabilities between the chiral selector in the stationary phase and the enantiomers to be separated (Alvarez-Rivera, Bueno, Ballesteros-Vivas, & Cifuentes, 2020). This method separates TAG enantiomers based on the spatial arrangement of the adsorbed FA chains.

Different chiral columns exhibit different separation effects. One study showed that a CHIRALCEL OD-RH column coated with cellulose-tris-(3,5-dimethylphenylcarbamate) on silica gel can separate *rac*-PPO, *rac*-OOP, and *rac*-PPL into their respective enantiomers. Using circular HPLC based on this chiral column and APCI-MS, the *sn*-OOP/*sn*-POO ratio in palm oil was determined to be approximately 3:2 (Nagai et al., 2011). This study was the first to achieve the separation of naturally occurring asymmetric TAG enantiomers. Further, this method is also suitable for analyzing the isomers of TAGs commonly found in fish and egg yolks (Nagai et al., 2013; Nagar et al., 2017). However, to discriminate between the peaks of *sn*-PPO and *sn*-OPP accurately, multiple treatments in a recirculating system are required, and this process requires up to 150 min. In contrast, when the CHIRALPAK IF-3 column equipped with an acetonitrile mobile phase was selected from various chiral columns to separate TAGs, a mixture of *sn*-PPO/*sn*-OPP/*sn*-POP was obtained within 30 min without recirculation in this HPLC system (Nagai et al., 2019). The TAG regioisomers and enantiomers in palm oil and lard were quantitatively analyzed using the same method (Nagai et al., 2020). In palm oil, the total content of *sn*-POP, *sn*-OPP, and *sn*-PPO was 22.9%, for which *sn*-POP was present in the highest content (19.0%), and the ratios of *sn*-PPO/*sn*-OPP and *sn*-OOP/*sn*-POO were approximately 1:1 and 3:2, respectively, which are consistent with the *sn*-OOP/*sn*-POO ratios detected in previous studies (Nagai et al., 2011). In lard, the total content of *sn*-OPO, *sn*-OOP, and *sn*-POO was 19.6%, among which *sn*-OPO exhibited the highest content (12.8%).

Lux Cellulose-1, a chiral chromatographic column coated with cellulose-tris-(3,5-dimethylphenylcarbamate) on silica gel, has been used to separate TAG enantiomers in human milk collected from different regions in China (Chen et al., 2020). Enantiomeric pairs, including *rac*-OPL1/*rac*-OPL2 and *rac*-PLO1/*rac*-PLO2, were successfully separated from the *rac*-OPL and *rac*-PLO standard products. However, only *rac*-OPL was successfully separated into *rac*-OPL1 and *rac*-OPL2 in human milk, whereas *rac*-PLO could not be separated into two enantiomers owing to its low content and difficulty in collection. This suggests that the sensitivity and selectivity of the method requires further optimization for certain TAG species. In future, novel chiral chromatographic packing materials and column materials could be developed to improve separation ability and selectivity for specific isomers. Two Lux Cellulose-1 columns were used in series to analyze the isomers of *sn*-OLO/*sn*-LOO/*sn*-OOL and *sn*-LLO/*sn*-OLL/*sn*-LOL in hazelnut oil and human plasma, and HPLC-APCI-MS was employed for quantification (Lisa & Holcapek, 2013).

The above study found that hexane and heptane showed identical effects in terms of the separation of the regioisomers of TAGs by Ag-HPLC, and heptane is less toxic than hexane (Gorska et al., 2023). Therefore, heptane and 2-propanol could also be investigated for the separation of TAG enantiomers in chiral columns in the future. Alternatively, a column filled with two stationary phases exhibited the effect of separation regioisomers and enantiomers, respectively, and paired with heptane and 2-propanol as mobile phases will be used to separate regioisomers and enantiomers TAGs, which may prove to be a good assumption (Fig. 3). In this system, the Ag⁺-exchanger at the front end of the column separates regioisomers, and cellulose-tris-(3,5-dimethylphenylcarbamate) at the back half of the column separates enantiomers. Notably, this system uses relatively safe solvents, which is particularly advantageous for laboratories and industries that must deal with large solvent quantities. Further, this dual system column can potentially separate both regioisomers and enantiomers of TAGs in a single run, which could significantly streamline the separation process. Finally, this method could eliminate the need for complex setups involving the multiple columns and valve interfaces that are typically required in two-dimensional chromatography. This can reduce the complexity of the chromatographic process, improve reproducibility, and decrease the potential for errors introduced by the interfaces.

Table 1
Overview of LC-MS methods for various TAGs isomers.

Samples	Chromatographic column specifications	Chromatographic conditions	Detection methods	Mass spectrometry conditions	Results	References
CIE shea olein CIE palm olein non-interesterified palm olein.	ChromSpher Lipids (4.6 mm i.d. × 250 mm, 5 μm)	Column temperature: 30 °C, injection volume: 10 μL, flow rate: 1 mL/min, mobile phase: heptane + acetonitrile + 2-propanol	Ag-HPLC/APCI-MS	Ion source temperature: 450 °C, capillary temperature: 250 °C, capillary voltage: 25.0 V, source voltage: 6.0 kV, <i>m/z</i> scanning range: 500–1000	<i>sn</i> -SOS/ <i>sn</i> -SSO, <i>sn</i> -POS/ <i>sn</i> -PSO, <i>sn</i> -POP/ <i>sn</i> -PPO, <i>sn</i> -SOO/ <i>sn</i> -OSO, <i>sn</i> -POO/ <i>sn</i> -OPO	(Gorska et al., 2023)
Confectionery oils	Luna SCX (2.0 mm i.d. × 150 mm, 5 μm)	Column temperature: 25 °C, injection volume: 10 μL, flow rate: 0.3 mL/min, mobile phase: <i>n</i> -heptane + ethyl acetate	Ag-HPLC/APCI-MS	Ion source temperature: 450 °C, capillary temperature: 250 °C, cone voltage: 25.0 V, <i>m/z</i> scanning range: 240–1000	<i>sn</i> -SOS/ <i>sn</i> -SSO, <i>sn</i> -POS/ <i>sn</i> -PSO, <i>sn</i> -POP/ <i>sn</i> -PPO, <i>sn</i> -SOO/ <i>sn</i> -OSO, <i>sn</i> -POO/ <i>sn</i> -OPO	(Santoro et al., 2018)
Sunflower oil lard	ChromSpher Lipids (4.6 mm i.d. × 250 mm, 5 μm)	Column temperature: 30 °C, injection volume: 1 μL, flow rate: 1 mL/min, mobile phase: hexane-2 + propanol + acetonitrile	Ag-HPLC/APCI-MS	Ion source temperature: 400 °C, drying gas temperature: 300 °C, nebulizing gas rate: 5 L/min, drying gas rate: 3 L/min, <i>m/z</i> scanning range: 50–1200	<i>sn</i> -POP/ <i>sn</i> -OPP, <i>sn</i> -OOP/ <i>sn</i> -OPO, <i>sn</i> -PLP/ <i>sn</i> -LPP, <i>sn</i> -LLP/ <i>sn</i> -LPL, <i>sn</i> -OLP/ <i>sn</i> -LOP/ <i>sn</i> -OPL	(Lísa, Velínská, & Holcapek, 2009)
Palm oil lard	CHIRALPAK IF-3 (4.6 mm i.d. × 250 mm, 3 μm)	Column temperature: 25 °C, injection volume: 10 μL, flow rate: 1.0 mL/min, mobile phase: acetonitrile	Chiral HPLC/ESI-MS	Ion source temperature: 120 °C, capillary voltage: 3 kV, cone voltage: 40 V, cone gas flow rate: 50 L/h, desolvation gas flow rate: 800 L/h, <i>m/z</i> scanning range: 300–1000	<i>sn</i> -PPO/ <i>sn</i> -OPP/ <i>sn</i> -POP, <i>sn</i> -OOP/ <i>sn</i> -POO/ <i>sn</i> -OPO	(Nagai et al., 2020)
Human milk	Lux Cellulose-1 (4.6 mm i.d. × 250 mm, 3 μm)	Column temperature: 30 °C, injection volume: 5 μL, flow rate: 0.5 mL/min, mobile phase: hexane + 2-propanol	Chiral HPLC/APCI-MS	Ion source temperature: 100 °C, probe temperature: 400 °C, MS multiplier voltage: 700 V, <i>m/z</i> scanning range: 200–1500	<i>rac</i> -OPL1/ <i>rac</i> -OPL2, <i>rac</i> -PLO1/ <i>rac</i> -PLO2	(Chen et al., 2020)
Hazelnut oil human plasma	Lux Cellulose-1 (4.6 mm i.d. × 250 mm, 3 μm)	Column temperature: 35 °C, injection volume: 1 μL, flow rate: 1 mL/min, mobile phase: hexane + 2-propanol	Chiral HPLC/APCI-MS	Ion source temperature: 400 °C, <i>m/z</i> scanning range: 50–1200	<i>sn</i> -OLO/ <i>sn</i> -LOO/ <i>sn</i> -OOL, <i>sn</i> -LLO/ <i>sn</i> -OLL / <i>sn</i> -LOL	(Lisa & Holcapek, 2013)
Palm oil	CHIRALCEL OD-RH (4.6 mm i.d. × 150 mm, 5 μm)	Column temperature: 25 °C, injection volume: 20 μL, flow rate: 0.5 mL/min, mobile phase: methanol	Chiral HPLC/APCI-MS	Ion source temperature: 120 °C, cone voltage: 20 V, cone gas flow rate: 50 L/h, desolvation gas flow rate: 200 L/h, <i>m/z</i> scanning range: 500–1000	<i>sn</i> -OOP/ <i>sn</i> -POO, <i>sn</i> -PPO/ <i>sn</i> -OPP, <i>sn</i> -PPL/ <i>sn</i> -LPP	(Nagai et al., 2011)
Sea buckthorn pulp oil	Ascentis C 18 (4.6 mm i.d. × 250 mm, 5 μm) CHIRALCEL OD-RH (4.6 mm i.d. × 150 mm, 5 μm) Zorbax Eclipse Plus C18 (2.1 mm i.d. × 100 mm, 1.8 μm)	Column temperature: 25 °C, injection volume: 20 μL, flow rate: 1 mL/min, mobile phase: acetonitrile + acetone	HPLC/ Chiral HPLC/APCI-MS	Ion source temperature: 120 °C, cone voltage: 30 V, cone gas flow rate: 47 L/h, desolvation gas flow rate: 250 L/h, <i>m/z</i> scanning range: 400–1000	<i>sn</i> -PoPoP/ <i>sn</i> -PPoPo, <i>sn</i> -PLP, <i>sn</i> -PPoP	(Kalpio et al., 2021)
Human milk	Varian ChromSpher 5 Lipids (4.6 mm i.d. × 250 mm, 5 μm) Zorbax Eclipse Plus C18 (2.1 mm i.d. × 100 mm, 1.8 μm)	Column temperature: 30 °C, injection volume: 5 μL, flow rate: 0.5 mL/min, mobile phase: hexane + hexane-2-propanol	HPLC/Ag-HPLC/APCI-MS	Ion source temperature: 100 °C, probe temperature: 400 °C, MS multiplier voltage: 700 V, <i>m/z</i> scanning range: 200–1500	<i>rac</i> -PPO/ <i>sn</i> -POP, <i>sn</i> -OPO/ <i>rac</i> -OOP, <i>rac</i> -LaOO/ <i>sn</i> -OLaO, <i>rac</i> -OPL/ <i>rac</i> -POL/ <i>rac</i> -PLO	(Chen et al., 2020)
Infant formulas	Varian ChromSpher 5 Lipids (4.6 mm i.d. × 250 mm, 5 μm) Zorbax Eclipse Plus C18 (4.6 mm i.d. × 150 mm, 5 μm)	Column temperature: 30 °C, injection volume: 5 μL, flow rate: 0.5 mL/min, mobile phase: dichloro-methane + acetone.	HPLC/Ag-HPLC/ESI-MS	Ion source temperature: 180 °C, source gas flow: 6 L/min, <i>m/z</i> scanning range: 50–1200	<i>rac</i> -PPO/ <i>sn</i> -POP, <i>sn</i> -OPO/ <i>rac</i> -OOP	(Chen et al., 2019)
Peanut oil	Varian ChromSpher 5 Lipids (4.6 mm i.d. × 150 mm, 5 μm)	Column temperature: 30 °C, injection volume: 10 μL, flow rate: 1.5 mL/min, mobile phase: hexane + acetonitrile	HPLC/Ag-HPLC/APCI-MS	Ion source temperature: 450 °C, declustering potential: 90 V, MS collision energy: 35 V–55 V, <i>m/z</i> scanning range: 500–1000	<i>rac</i> -PLO/ <i>rac</i> -POL, <i>rac</i> -POP/ <i>rac</i> -PPO, <i>rac</i> -POO/ <i>rac</i> -OPO	(Hu et al., 2013)
Human milk, cow milk, infant formula, palm oil, sunflower oil	Phenomenex Kinetex C18 (3 mm i.d. × 100 mm, 3 μm)	Column temperature: 30 °C, flow rate: 0.3 mL/min, mobile phase: methanol+acetonitrile + H ₂ O + ammonium acetate)	LC-MS/MS	Ion source temperature: 550 °C, spray voltage: 5500 V, collision energy: 10 V–45 V, electron kinetic energy: 15 eV, electron beam current: 6000 nA, scanning range: 200–1000	<i>sn</i> -OPO/ <i>sn</i> -POO, <i>sn</i> -PLO/ <i>sn</i> -POL/ <i>sn</i> -OPL, <i>sn</i> -LPL	(Zhang et al., 2024)

(continued on next page)

Table 1 (continued)

Samples	Chromatographic column specifications	Chromatographic conditions	Detection methods	Mass spectrometry conditions	Results	References
Human milk	Cortecs C18 column (2.1 mm i.d. × 150 mm, 1.6 μm)	Column temperature: 60 °C, flow rate: 0.2–0.3 mL/min, mobile phase: methanol (ammonium acetate) + 2-propanol	UHPLC-ESI-MS/MS	Ion source temperature: 120 °C, capillary voltage: 4.9 kV, cone voltage: 22 V, cone gas flow rate: 200 L/h, desolvation gas flow rate: 750 L/h, m/z scanning range: 100–700	<i>sn</i> -OPO, <i>sn</i> -OPL/ <i>sn</i> -OLP/ <i>sn</i> -POL, <i>sn</i> -OPLa/ <i>sn</i> -OLaP/ <i>sn</i> -POLa, <i>sn</i> -PSO/ <i>sn</i> -POS/ <i>sn</i> -OPS	(Sazzad et al., 2022)
Bovine milk	Acclaim C30 (3 mm i.d. × 250 mm, 3 μm)	Column temperature: 30 °C, injection volume: 5 μL, flow rate: 0.45 mL/min, mobile phase: acetonitrile	LC-MS	Ion source temperature: 300 °C, capillary temperature: 300 °C, m/z scanning range: 120–1200	<i>sn</i> -OPO/ <i>sn</i> -OOP, <i>sn</i> -OSO/ <i>sn</i> -OOS	(Liu & Rochfort, 2021)
Human milk	BEH C18 (2.1 mm i.d. × 100 mm, 1.7 μm)	Column temperature: 25 °C, flow rate: 0.2 mL/min, mobile phase: methanol + isopropanol	UPLC-MS/MS	Ion source temperature: 100 °C, capillary voltage: 3 kV, cone voltage: 40 V, cone gas flow rate: 60 L/h, desolvation gas flow rate: 700 L/h, m/z scanning range: 600–1000	<i>rac</i> -OPLa/ <i>rac</i> -OLaP, <i>sn</i> -OLaO/ <i>rac</i> -OLOa, <i>rac</i> -LOO/ <i>sn</i> -OLO, <i>rac</i> -LPO/ <i>rac</i> -OLP, <i>sn</i> -OPO, <i>rac</i> -OPP, <i>rac</i> -OPS	(Kallio et al., 2017)

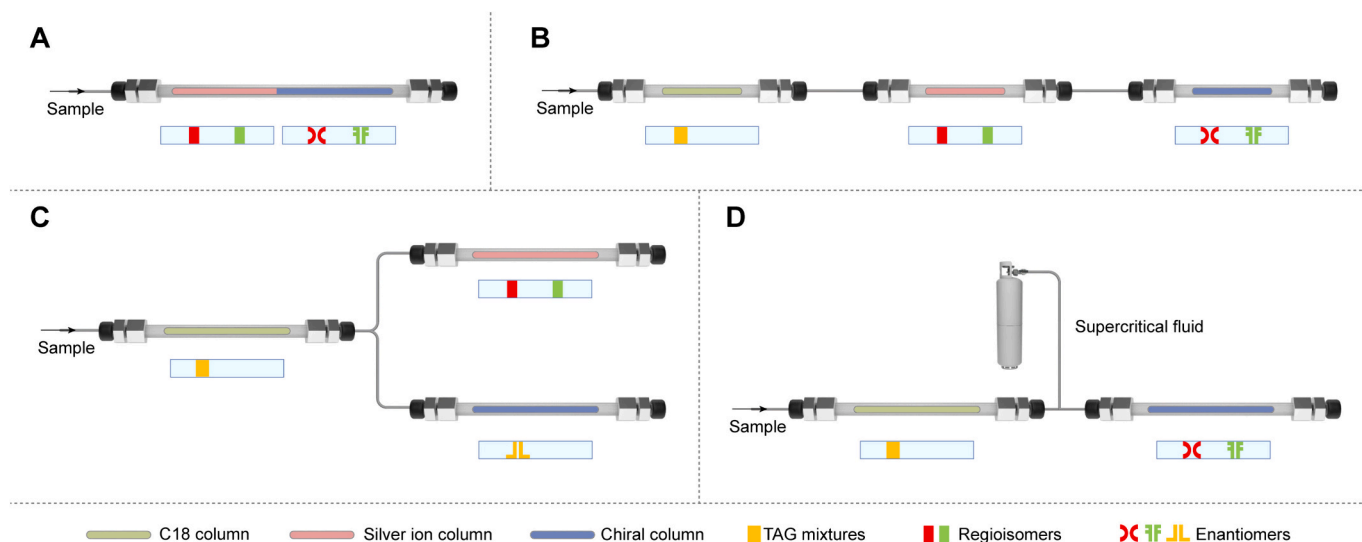


Fig. 3. Schematic diagram of separation and identification of regioisomers and enantiomers. (A) Silver ion-chiral chromatographic columns. (B) Three-dimensional chromatographic columns in series. (C) Tandem and parallel columns. (D) Supercritical carbon dioxide coupled with C18 column and chiral column.

3.3.1.3. Two-dimensional chromatographic columns. Although some TAG isomers can be analyzed using Ag^+ and chiral chromatographic columns, there is a lack of general column-solvent combinations for completely separating TAG isomers from mixtures (Ali, Suhail, & Aboul-Enein, 2019). To separate more types of TAG isomers and determine the ratio of target TAG isomers, a two-dimensional chromatographic system has been developed. By employing two-dimensional chromatography, the researchers could first use one column (a positive-phase column) to separate compounds based on polarity. Subsequently, the eluate from the first dimensional column is introduced into a second dimensional column (e.g., negative-phase column) to perform secondary separation based on different interactions using different stationary phases. (Cacciola, Donato, Sciarrone, Dugo, & Mondello, 2017). Two-dimensional chromatography is widely used in analytical chemistry because it can fully utilize the advantages of both positive phase- and negative-phase chromatography to achieve high-resolution separations.

An LC × LC system composed of a Zorbax Eclipse Plus C18 column and a Varian ChromSpher 5 Lipids Ag^+ chromatographic column was used to analyze the regioisomers of OPO and PPO in infant formulas quantitatively (Chen et al., 2019). The components corresponding to OPO and PPO were collected through the Zorbax column in the first

dimension and then passed into the second-dimension Varian column to separate the regioisomers of OPO and PPO. The major structured TAGs in infant formulas containing *sn*-OPO were found to be *sn*-OPO (approximately 70%) and *rac*-PPO (> 95%). However, *rac*-OOP (65.24–100%) and *sn*-POP (about 90%) were the major structured TAGs in infant formulas without *sn*-OPO. Subsequently, the same method was used to isolate and characterize the regioisomers of human milk TAGs composed of lauric acid (La), oleic acid, palmitic acid, and linoleic acid (including nine regioisomers: *rac*-PPO/*sn*-POP, *sn*-OPO/*rac*-OOP, *rac*-LaOO/*sn*-OLaO, and *rac*-OPL/*rac*-POL/*rac*-PLO), and their relative contents were calculated (Chen et al., 2020). The enantiomeric fraction of asymmetric TAGs extracted from sea buckthorn pulp oil was analyzed using two-dimensional chromatography consisting of an Ascentis C18 column and a CHIRALCEL OD-RH column combined with APCI-MS (Kalpio, Linderborg, Fabritius, Kallio, & Yang, 2021). In sea buckthorn oil, the TAGs composed of palmitoleic acid (Po) and palmitic acid were mainly *sn*-PoPoP and *sn*-PPoP, which is consistent with earlier findings indicating that palmitic acid is mainly located at the *sn*-1 or *sn*-3 position (Yang & Kallio, 2006).

On the basis of the above findings, the combination of a C18 column with an Ag^+ column or a chiral column enables the separation and

detection of target TAG components more rapidly and efficiently than using only an Ag^+ column or a chiral column. This strategy of combining columns effectively reduces interference from other TAG components, thereby significantly improving the resolution and number of TAG isomers detected. Thus, a C18 column can be connected to Ag^+ and chiral chromatography columns to separate both regioisomers and enantiomers (Fig. 3). This setup enables the full analysis of the sample in a single experimental run. Alternatively, a C18 column can be used to collect the target fractions, which are then analyzed separately using Ag^+ and chiral chromatography columns (Fig. 3). This approach facilitates a more targeted analysis, focusing on specific regioisomers or enantiomers of interest.

3.3.2. Ion fragmentation methods

Because C18 columns can only separate TAG species and not their isomers, the isomer species must be determined from ion fragments. The corresponding secondary mass spectra can be extracted from the total ion chromatogram using the precursor ions ($[\text{M} + \text{NH}_4]^+$) of TAGs and DAGs, and the FA species on the glycerol backbone deduced from the $[\text{M} + \text{H-FA}]^+$ fragment ions can then be determined (Liu et al., 2022). In fact, the ester bonds at *sn*-1 and *sn*-3 in TAGs are more easily broken than that at *sn*-2, resulting in different abundances of $[\text{M} + \text{H-FA}]^+$. Therefore, different types of regioisomers can be identified according to the different fragment intensities (Zhang, Wei, Tao, Jin, & Wang, 2022).

Tandem MS has been used to obtain additional structural information regarding the molecular and fragment ions. Most existing tandem MS methods adopt collision-induced dissociation (CID) to generate fragment ions. However, the DAG ions produced can only identify TAG isomers having the same molecular weight but different fatty acyls, the regioisomers and enantiomers cannot be identified. Thus, researchers have used the intensity of DAG fragment ions to build calibration curves for the identification and relative quantification of target TAGs regioisomers (Leveque, Acheampong, Heron, & Tchaplal, 2012; Liu & Rochfort, 2021). Regioisomer standards with different concentrations and ratios were analyzed by Tarvainen, Kallio, and Yang (2019), who used the $[\text{R}_A\text{R}_B]^+ / [\text{R}_A\text{R}_A]^+$ ratio and the *sn*-ABA content (%) to establish regioisomer calibration curves of 18 AAB/ABA-type regioisomer pairs. Notably, the ratio of $[\text{R}_A\text{R}_C]^+ / ([\text{R}_A\text{R}_B]^+ + [\text{R}_A\text{R}_C]^+ + [\text{R}_B\text{R}_C]^+)$ and the *sn*-2 FA content (%) were first used to establish calibration curves of the five ABC-types regioisomers TAGs, which provided a new theoretical basis for the quantitative analysis of TAG regioisomers in natural oils and fats. A similar method was adopted by Zhang et al. (2022) using the $[\text{R}_A\text{R}_B]^+ / ([\text{R}_A\text{R}_A]^+ + [\text{R}_A\text{R}_B]^+)$ ratio and the *sn*-ABA content (%) for calibration curves. In addition, the research group introduced a correction factor for ^{13}C isotope effects to minimize errors during the experiment, and this correction method is essential to improve the accuracy of the analytical results. The theoretical equations for calculating the regional isomers were also summarized, and the contents of OPLA, OPP, OPO and OPL triglyceride regional isomers in human and animal milk were calculated using the theoretical equations and calibration curves, which proved the validity of the method in the analysis of real samples.

The presence of multiple TAGs with the same molecular weight in complex samples generates multiple overlapping fragment ions, which affects the target fragment ion ratio and complicates manual calculations. Therefore, advanced data processing tools and software have been developed to simplify the process of producing calibration curves and calculating regioisomer content. Linderborg et al. (2014) used two computational methods to quantify TAG regioisomers in the human milk of mothers with different dietary intakes and pre-pregnancy body mass indices. One method involved establishing a calibration curve between the $[\text{R}_A\text{R}_B]^+ / ([\text{R}_A\text{R}_A]^+ + [\text{R}_A\text{R}_B]^+)$ ratio and *sn*-ABA content, and in the other, calculations were performed using MSPECTRA in negative ion mode. The ratio of *sn*-POO + *sn*-OOP calculated using MSPECTRA was $0.5 \pm 1.0\%$, whereas the calibration curve yielded a considerably higher ratio of $14.6 \pm 5.5\%$ because it failed to distinguish whether DAG

fragments with the same mass (36:2) were derived from POO or LPS. A previous direct injection tandem MS method for analyzing TAG regioisomers was recently modified (Fabritius et al., 2020), and the ratios of TAG regioisomers were calculated based on the abundance of $[\text{M-H-FA-100}]^-$ and $[\text{RCOO}]^-$ ions using MSPECTRA. A total of 241 regioisomers (including *sn*-PLO/*sn*-LPO/*sn*-POL and *sn*-OOP/*sn*-OPO) in human milk, bovine milk, and infant formula from China and Finland were quantified using this method. In addition to MSPECTRA, Kallio, Nylund, Bostrom, and Yang (2017) used an optimized algorithm running on GNU Octave 4.0.0 to analyze regioisomers in Chinese and Finnish human milk samples. The results showed that the highest TAG content in Finnish samples was *sn*-OPO, whereas the highest TAG content in Chinese samples was *rac*-OPL. The relatively high OPL content of the human milk from China is associated with the relatively high intake of linoleic acid in the country (Yu et al., 2022).

Subsequently, Sazzad et al. (2022) optimized the aforementioned algorithm based on MSPECTRA, established an internal fragment model using TAG standards, and considered the difference in the cracking efficiency of different TAG substances. This new computational program was combined with the ultra-high-performance liquid chromatography electrospray ionization tandem mass spectrometry (UHPLC-ESI-MS/MS) method to analyze the contents of *sn*-OPO, *sn*-LPL, *sn*-OPL, and *sn*-OPS in human milk, and the results were similar to those reported previously (Fabritius et al., 2020). Compared with earlier programs, the new program features a higher throughput, faster calculation speed, and more accurate analysis of TAGs having the same molecular weight. However, this method has a limitation: the program is accurate for high abundance TAGs, but the accuracy decreases as the relative proportion of TAGs decreases. Therefore, future research should first focus on improving relevant algorithms to better handle data analysis of low-abundance TAGs. This may include enhancing signal processing capabilities, optimizing background noise filtering strategies, and optimizing data processing flow. Second, algorithms and models tailored for low-abundance TAGs should be developed using advanced statistical principles or deep learning frameworks. Finally, a mechanism for integrating multi-source data from different platforms and experimental conditions should be identified to improve the accuracy of analyzing low-abundance TAGs.

To quantify TAG regioisomers for which no standards are commercially available, Balgoma et al. (2019) analyzed published data on the cleavage patterns of TAG regioisomers and the effect of cleavage energy on the TAG cleavage patterns. Based on the esterification position and structure of FAs and their mutual interactions, the common fragmentation trend in each dataset was modeled, and the TAG regioisomers in sunflower and olive oils were quantitatively analyzed using the established model. The TAG isomers in plant oils were found to be mainly present in the forms of *sn*-POP, *sn*-PLP, *rac*-POS, *rac*-OOP, *rac*-POL, and *rac*-PLO, and the quantitative results were consistent with those of TAGs isomers in the existing literature (Pchelkin, Kuznetsova, Tsydendambaev, & Vereshchagin, 2001).

Notably, electron-activated dissociation (EAD) can provide fragment ion information complementary to CID, thereby improving the analysis of TAG isomers. Depending on the electron energy, the EAD fragmentation modes are divided into electron capture dissociation (ECD, 0–5 eV), hot ECD (5–10 eV), and electron impact excitation of ions from organic compounds (EIEIO, >10 eV). EIEIO causes TAGs to produce a region of loss of the diacyl chain, wherein the region exhibits single peaks that identify FAs at the *sn*-2 position and double peaks that identify FAs at the *sn*-1 and *sn*-3 positions. In addition, according to the characteristics of EAD that breaks single but not double bonds, the position of double bonds in the fatty acid chain can be determined. (Baba, Campbell, Le Blanc, & Baker, 2016). The SCIEX ZenofTOF™7600 system combines EAD and CID technology to produce more characteristic fragment ions on radical fragments, providing a new dimension for mass spectrometry studies. Zhang et al. (2024) established a standard curve based on this device using the relationship between the peak area of the characteristic fragment ion at the *sn*-2 position and the content of the

TAG recombinant isomer standard, which improves analytical efficiency and ensures quantitative accuracy. The research team used this method to quantify TAG isomers in human milk, cow milk, infant formula, palm oil, and sunflower oil and to determine the double bond positions of UFAs. The results showed that human milk contained 60.58, 3.19, 6.09, 68.70, and 0.96 $\mu\text{g}/\text{mg}$ of *sn*-OPL, *sn*-POL, *sn*-PLO, *sn*-OPO, and *sn*-POO, respectively. This compositional ratio is consistent with the findings of Zhang et al. (2022). In particular, the main difference between infant formula and breast milk was the *sn*-OPL content. This difference may stem from the use of vegetable oils as a source of TAG in infant formulas. Thus, these findings suggest that manufacturers of infant formula should consider increasing the content of *sn*-OPL or using animal milk fat as an ingredient in future production to resemble the composition of human milk more closely and better meet the nutritional needs of infants and young children. In addition, the SCIEX ZenoTOF™7600 system uses the Zeno™ trap technology to obtain high-quality secondary high-resolution MS data from very low-concentration samples, combined with optimized algorithms to obtain relevant structural information for low-abundance TAGs quickly and accurately. However, current techniques are unable to distinguish enantiomers. Therefore, the development of new rupture modes to obtain the secondary characteristic fragment ions of *sn*-1 and *sn*-3, or based on the collection of secondary fragment ions, fragmentation and cracking are performed again to analyze tertiary fragment ions, which accurately identify the types of FAs connected at the *sn*-1,3 position of TAGs; and is a research direction for isomer analysis using mass spectrometry.

3.4. Supercritical fluid chromatography method

Supercritical fluid chromatography (SFC) was developed in the 1980s. Because the viscosities and diffusion coefficients of supercritical fluids are very close to those of gases, supercritical fluids having high mobile phase speeds can achieve a high separation efficiency (Tyskiewicz, Debczak, Gieysztor, Szymczak, & Roj, 2018). At the same time, the densities and diffusivities of supercritical fluids are similar to those of liquids, thus providing good analyte solubility (Yang et al., 2019). SFC has characteristics of both gas and liquid chromatography, which may help achieve a higher analysis efficiency compared to that of ordinary liquid-phase systems (Yang et al., 2017).

In recent years, SFC has been increasingly applied in the field of lipidomics (Takeda et al., 2018). For example, a quantitative method for determining TAG regioisomers and enantiomers was developed by Masuda, Abe, and Murano (2021). Three isomers (*sn*-POO, *sn*-OPO, and *sn*-OOP) were identified by SFC-Q-MS with a CHIRALPAK IG-U column. Meanwhile, a calibration curve was established to analyze the contents of *sn*-OPO, *sn*-POO, and *sn*-OOP in extra-virgin olive oil, refined olive oil, palm oil, palm oleoresin, and esterified palm oleoresin quantitatively. However, this method could not isolate the regioisomers and enantiomeric isomers of TAGs that only contain saturated FAs. Ultra-performance SFC with quadrupole time-of-flight mass spectrometry (UPSFC-Q-TOF-MS) used to analyze isomers with supercritical carbon dioxide as the mobile phase and BEH-2EP column. Using this method, the compositions of isomers in human milk at different lactations periods, infant formulas using different fat sources, other mammalian milk, and plant oils were analyzed (Zhang et al., 2021). The results showed that the *sn*-OPO regioisomer accounted for >80% of the total OPO in human milk, whereas the *sn*-OOP content was higher in the other samples. The same research team also used this method to separate and quantify TAG regioisomers containing palmitic acid in human milk, bovine milk, lard, and fish oil, and they performed a quantitative analysis using a calibration curve and calculations (Zhang et al., 2022). In terms of content, the top three regioisomers in human milk were *sn*-OPL, *sn*-OPO, and *sn*-LPL, for which the *sn*-2 palmitate TAGs accounted for >50% of TAGs. Lard and fish oil were similar to human milk, and they also contained a large amount of palmitic acid at the *sn*-2 position. The content of palmitic acid at the *sn*-2 position in bovine milk was higher

than that in plant oils, but it was still significantly lower than that in human milk.

The combination of HPLC and SFC offers a powerful analytical tool for the separation and analysis of complex lipid mixtures such as those found in human milk. Because of the unique characteristics of each chromatographic technique, the use of a C18 column in tandem with a chiral column, as well as supercritical carbon dioxide as the mobile phase (Fig. 3) is promising. This combination technique utilizes the separation mechanisms of the different columns to achieve the high-resolution analysis of TAG isomers in complex samples through a multi-step separation process; the mobile nature of supercritical carbon dioxide helps speed up the analysis process, allowing for rapid chromatographic analysis. A previous study used SFC coupled with ion-mobility MS to analyze TAG isomers (Xia et al., 2021), but its application to the analysis of human milk samples presents challenges and requires the development and optimization of sample extraction methods, as well as the adjustment of instrumental parameters to ensure that TAG isomers can be accurately detected and analyzed in human milk.

3.5. Nuclear magnetic resonance (NMR) methods

In NMR systems, the magnetic moment of a nucleus in the low-energy state absorbs the energy resulting from the interactions of constant and alternating magnetic fields, resulting in a transition to a high-energy state, which produces NMR signals (Kruk et al., 2017). NMR systems do not have the same sensitivity as chromatographic systems, but they can quickly provide structural and compositional information about TAG mixtures in oils without specific sample preparation. Compared to chromatographic analysis, NMR can determine the total TAG content and total SFA/UFA ratio with a shorter acquisition time (Indelicato et al., 2017). For example, a previous study obtained quantitative data on the composition and regioisomer distribution of all major UFAs of TAGs in pork and beef using ^{13}C NMR (Kildahl-Andersen, Gjerlaug-Enger, Rise, Haug, & Egelandsdal, 2021). This analysis method involved the manual integration of carbonyl signal peaks to determine the ratio of SFAs and UFAs at the *sn*-1,3 and *sn*-2 positions. This system not only quantified the monounsaturated FAs present in beef and pork TAG extracts and the overall amount of SFAs but also provided the regioisomerization distribution of UFAs on the glycerol skeleton. Furthermore, this method could independently quantify the concentrations of palmitic acid and stearic acid in pork TAGs, including the regioisomer distributions. The carbonyl region of the ^{13}C NMR spectra is suitable for distinguishing SFAs from UFAs, including the distribution of FAs in terms of regional positions on the TAGs. Therefore, ^{13}C NMR has a unique advantage in providing information on the distribution of FA positions between the triglyceride *sn*-1,3 and *sn*-2 positions, as well as the overall composition.

Although all the aforementioned methods may be used to detect TAG isomers, they have different characteristics (Table 2). Enzymatic hydrolysis is relatively simple, and it separates FAs at the *sn*-1,3 position from the glycerol backbone and the FAs and *sn*-2 monoacylglycerols in subsequent individual analyses. However, it can only obtain the distribution information of FAs in the *sn*-1,3 and *sn*-2 positions of triglycerides, and acyl migration reaction may occur during hydrolysis, resulting in an inaccurate FA distribution. LC-MS, which is the primary method for analyzing TAG isomers, enables the qualitative and quantitative analysis of several major isomers in human milk. Chiral LC-MS is often used to analyze the enantiomers, but this process can require cycling, making it time-consuming. SFC can improve upon the chromatographic separation efficiency of these systems owing to the high diffusivity and low viscosity of supercritical fluids, making the separation and purification of samples faster and more efficient. In addition, because supercritical fluids do not contain volatile organic solvents, less chemical waste and pollution are generated. However, SFC reagents and equipment are relatively expensive. In contrast, the NMR method does not require sample pretreatment, but it does require specialized

Table 2
Characteristics of common methods for detecting TAG isomers.

Methods	Characteristics	References
Enzymatic hydrolysis	Simple and convenient operation Inexpensive instrumentation Low accuracy Cannot yield structural information on individual TAG regioisomers	(Deng et al., 2018; Qi et al., 2018)
GC-MS	Less organic reagent required Relatively simple instrument operation Poor stability Prone to acyl traverse and thermal decomposition	(Garcés et al., 2023)
LC-MS	Broader applications Analysis of key isomers in human milk Time-consuming Expensive instrumentation	(Chen et al., 2020; Liu & Rochfort, 2021; Nagai et al., 2020; Santoro et al., 2018; Zhang et al., 2022)
SFC	Short run times Very low environmental load Not applicable to isomers containing only saturated FAs Expensive instrumentation and reagents	(Masuda et al., 2021; Zhang et al., 2021, 2022)
NMR	No preprocessing required Can directly extract location information of unsaturated components Low sensitivity Expensive instrumentation	(Kildahl-Andersen et al., 2021)

equipment and technical support, which increase costs. In future work, different methods may be combined to obtain extensive information regarding the structures of TAG isomers.

4. Summary and outlook

The TAG isomers in human milk can be qualitatively or quantitatively analyzed using enzymatic hydrolysis, GC-MS, LC-MS, SFC, and ¹³C NMR, with LC-MS being particularly common. Additionally, automatic calculations have been developed to analyze TAG isomers accurately and quickly. Although existing methods can partially separate the regional and enantiomeric isomers of human milk TAGs (such as OPO, OPL, and LaOO), most isomer TAGs cannot be analyzed. Because chromatographic separation is limited to certain specific isomers, MS does not provide adequate fragmentation information to determine the isomer species accurately, and the composition of human milk is too complex to apply some of the currently used analytical methods directly. Thus, the comprehensive analysis of TAG isomers in human milk is challenging.

To improve the separation and identification of TAG isomers, future research should focus on several different approaches, such as using new chromatographic combinations, optimizing existing techniques, and developing high-sensitivity and high-resolution instrumentation. The comprehensive identification of TAG isomers in human milk is essential for understanding their nutritional impact on infants. By employing these analytical techniques, researchers can better characterize the complex lipid profile of human milk. This will contribute to the development of lipids for infant formula that mimic the structure and function of those in human milk and infant nutrition products that support the health and development of infants.

CRediT authorship contribution statement

Huiru Cao: Data curation, Formal analysis, Visualization, Writing – original draft, Writing – review & editing. **Qian Liu:** Conceptualization, Software, Writing – review & editing. **Yan Liu (刘妍):**

Visualization, Writing – review & editing. **Junyong Zhao:** Investigation. **Weicang Qiao:** Project administration. **Yuru Wang:** Validation. **Yan Liu (刘言):** Data curation. **Lijun Chen:** Project administration, Supervision, Funding acquisition.

Declaration of competing interest

The authors declare that they have no known competing financial interests or personal relationships that could have appeared to influence the work reported in this paper.

Data availability

Data will be made available on request.

Acknowledgements

National Natural Science Foundation of China (Grant No. 32272316), Beijing Innovation Team of Livestock Industry Technology System, Beijing Science and Technology Plan (Grant No. Z221100006422012).

References

- Abdi Hasibuan, H. A., Sitanggang, A. B., Andarwulan, N., & Hariyadi, P. (2021). Enzymatic synthesis of human Milk fat substitute—A review on technological approaches. *Food Technology and Biotechnology*, 59(4), 475–495. <https://doi.org/10.17113/ftb.59.04.21.7205>
- Ali, I., Suhail, M., & Aboul-Enein, H. Y. (2019). Advances in chiral multidimensional liquid chromatography. *TrAC Trends in Analytical Chemistry*, 120, Article 115634. <https://doi.org/10.1016/j.trac.2019.115634>
- Alvarez-Rivera, G., Bueno, M., Ballesteros-Vivas, D., & Cifuentes, A. (2020). Chiral analysis in food science. *TrAC Trends in Analytical Chemistry*, 123, Article 115761. <https://doi.org/10.1016/j.trac.2019.115761>
- Arena, P., Sciarone, D., Dugo, P., & Mondello, L. (2021). Pattern-type separation of Triacylglycerols by silver thiolate×non-aqueous reversed phase comprehensive liquid chromatography. *Separations*, 8(6), 88. <https://doi.org/10.3390/separations8060088>
- Baba, T., Campbell, J. L., Le Blanc, J. C. Y., & Baker, P. R. S. (2016). Structural identification of triacylglycerol isomers using electron impact excitation of ions from organics (EIEIO). *Journal of Lipid Research*, 57(11), 2015–2027. <https://doi.org/10.1194/jlr.M070177>
- Bakala-N'Goma, J.-C., Couédelo, L., Vaysse, C., Letisse, M., Pierre, V., Géloin, A., ... Carrière, F. (2022). The digestion of diacylglycerol isomers by gastric and pancreatic lipases and its impact on the metabolic pathways for TAG re-synthesis in enterocytes. *Biochimie*, 203, 106–117. <https://doi.org/10.1016/j.biochi.2022.01.003>
- Balgoma, D., Guitton, Y., Evans, J. J., Le Bizec, B., Dervilly-Pinel, G., & Meynier, A. (2019). Modeling the fragmentation patterns of triacylglycerides in mass spectrometry allows the quantification of the regioisomers with a minimal number of standards. *Analytica Chimica Acta*, 1057, 60–69. <https://doi.org/10.1016/j.aca.2019.01.017>
- Béghin, L., Marchandise, X., Lien, E., Bricout, M., Bernet, J.-P., Lienhardt, J.-F., Jeannerot, F., Menet, V., Requillart, J.-C., Marx, J., De Groot, N., Jaeger, J., Steenhout, P., & Turck, D. (2019). Growth, stool consistency and bone mineral content in healthy term infants fed sn-2-palmitate-enriched starter infant formula: A randomized, double-blind, multicentre clinical trial. *Clinical Nutrition*, 38(3), 1023–1030. <https://doi.org/10.1016/j.clnu.2018.05.015>
- Bourliet, C., Menard, O., De La Chevasserie, A., Sams, L., Rousseau, F., Madec, M.-N., Robert, B., Deglaire, A., Pezenneec, S., Bouhallab, S., Carrière, F., & Dupont, D. (2015). The structure of infant formulas impacts their lipolysis, proteolysis and disintegration during in vitro gastric digestion. *Food Chemistry*, 182, 224–235. <https://doi.org/10.1016/j.foodchem.2015.03.001>
- Cacciola, F., Donato, P., Sciarone, D., Dugo, P., & Mondello, L. (2017). Comprehensive liquid chromatography and other liquid-based comprehensive techniques coupled to mass spectrometry in food analysis. *Analytical Chemistry*, 89(1), 414–429. <https://doi.org/10.1021/acs.analchem.6b04370>
- Chen, Q., Xie, Q., Jiang, C., Evvie, S. E., Cao, T., Wang, Z., ... Huo, G. (2022). Infant formula supplemented with 1,3-olein-2-palmitin regulated the immunity, gut microbiota, and metabolites of mice colonized by feces from healthy infants. *Journal of Dairy Science*, 105(8), 6405–6421. <https://doi.org/10.3168/jds.2021-21736>
- Chen, Y., Zhang, X., Li, D., Yi, H., Xu, T., Li, S., & Zhang, L. (2019). Fatty acid and triacylglycerol comparison of infant formulas on the Chinese market. *International Dairy Journal*, 95, 35–43. <https://doi.org/10.1016/j.idairyj.2019.02.017>
- Chen, Y. J., Zhou, X. H., Han, B., Yu, Z., & Zhang, L. W. (2020). Regioisomeric and enantiomeric analysis of primary triglycerides in human milk by silver ion and chiral HPLC APCI-MS. *Journal of Dairy Science*, 103(9). <https://doi.org/10.3168/jds.2019-17353>
- Choi, Y., & Chang, P.-S. (2022). Kinetic modeling of lipase-catalysed hydrolysis of triacylglycerol in a reverse micelle system for the determination of integral

- stereoselectivity. *Catalysis Science & Technology*, 12(9), 2819–2828. <https://doi.org/10.1039/D1CY02182F>
- Choi, Y., Park, J.-Y., & Chang, P.-S. (2021). Integral Stereoselectivity of lipase based on the chromatographic resolution of enantiomeric/Regioisomeric diacylglycerols. *Journal of Agricultural and Food Chemistry*, 69(1), 325–331. <https://doi.org/10.1021/acs.jafc.0c07430>
- Dean, D. C., Dirks, H., O'Muirheartaigh, J., Walker, L., Jersky, B. A., Lehman, K., ... Deoni, S. C. L. (2014). Pediatric neuroimaging using magnetic resonance imaging during non-sedated sleep. *Pediatric Radiology*, 44(1), 64–72. <https://doi.org/10.1007/s00247-013-2752-8>
- Deng, L., Zou, Q., Liu, B., Ye, W., Zhuo, C., Chen, L., Deng, Z.-Y., Fan, Y.-W., & Li, J. (2018). Fatty acid positional distribution in colostrum and mature milk of women living in Inner Mongolia, North Jiangsu and Guangxi of China. *Food & Function*, 9(8), 4234–4245. <https://doi.org/10.1039/c8fo00787j>
- Fabritius, M., Linderborg, K. M., Tarvainen, M., Kalpio, M., Zhang, Y., & Yang, B. (2020). Direct inlet negative ion chemical ionization tandem mass spectrometry analysis of triacylglycerol regioisomers in human milk and infant formulas. *Food Chemistry*, 328, Article 126991. <https://doi.org/10.1016/j.foodchem.2020.126991>
- Garcés, R., Martínez-Force, E., Venegas-Calerón, M., Moreno-Pérez, A. J., & Salas, J. J. (2023). A GC/MS method for the rapid determination of disaturated triacylglycerol positional isomers. *Food Chemistry*, 409, Article 135291. <https://doi.org/10.1016/j.foodchem.2022.135291>
- Gorska, A., Salgarella, N., Calaminici, R., Forte, E., Beccaria, M., & Purcaro, G. (2023). Impact of column temperature on triacylglycerol regioisomers separation in silver ion liquid chromatography using heptane-based mobile phases. *Journal of Chromatography A*, 1702, Article 464095. <https://doi.org/10.1016/j.chroma.2023.464095>
- Guo, D., Li, F., Zhao, J., Zhang, H., Liu, B., Pan, J., Zhang, W., Chen, W., Xu, Y., Jiang, S., & Zhai, Q. (2022). Effect of an infant formula containing sn-2 palmitate on fecal microbiota and metabolite profiles of healthy term infants: A randomized, double-blind, parallel, controlled study. *Food & Function*, 13(4), 2003–2018. <https://doi.org/10.1039/d1fo03692k>
- Hageman, J. H. J., Danielsen, M., Nieuwenhuizen, A. G., Feitsma, A. L., & Dalsgaard, T. K. (2019). Comparison of bovine milk fat and vegetable fat for infant formula: Implications for infant health. *International Dairy Journal*, 92, 37–49. <https://doi.org/10.1016/j.idairyj.2019.01.005>
- Holapek, M., & Lisa, M. (2017). Silver-Ion liquid chromatography–mass spectrometry—sciencedirect. In *Handbook of Advanced Chromatography/Mass Spectrometry Techniques* (pp. 115–140).
- Hou, A., Xiao, Y., & Li, Z. (2019). Effects of 1, 3-dioleoyl-2-palmitoylglycerol and its plant-oil formula on the toddler fecal microbiota during in vitro fermentation. *CyTA Journal of Food*, 17(1), 850–863. <https://doi.org/10.1080/19476337.2019.1648555>
- Hu, J., Wei, F., Dong, X.-Y., Lv, X., Jiang, M.-L., Li, G.-M., & Chen, H. (2013). Characterization and quantification of triacylglycerols in peanut oil by off-line comprehensive two-dimensional liquid chromatography coupled with atmospheric pressure chemical ionization mass spectrometry. *Journal of Separation Science*, 36(2), 288–300. <https://doi.org/10.1002/jssc.201200567>
- Indelicato, S., Bongiorno, D., Pitzonzo, R., Di Stefano, V., Calabrese, V., Indelicato, S., & Avellone, G. (2017). Triacylglycerols in edible oils: Determination, characterization, quantitation, chemometric approach and evaluation of adulterations. *Journal of Chromatography A*, 1515, 1–16. <https://doi.org/10.1016/j.chroma.2017.08.002>
- Jakaitis, B. M., & Denning, P. W. (2014). Human breast milk and the gastrointestinal innate immune system. *Clinics in Perinatology*, 41(2), 423–435. <https://doi.org/10.1016/j.clp.2014.02.011>
- Jiang, T., Liu, B., Li, J., Dong, X., Lin, M., Zhang, M., Zhao, J., Dai, Y., & Chen, L. (2018). Association between sn-2 fatty acid profiles of breast milk and development of the infant intestinal microbiome. *Food & Function*, 9(2), 1028–1037. <https://doi.org/10.1039/c7fo00088j>
- Kallio, H., Nylund, M., Bostrom, P., & Yang, B. (2017). Triacylglycerol regioisomers in human milk resolved with an algorithmic novel electrospray ionization tandem mass spectrometry method. *Food Chemistry*, 233, 351–360. <https://doi.org/10.1016/j.foodchem.2017.04.122>
- Kalpio, M., Linderborg, K. M., Fabritius, M., Kallio, H., & Yang, B. (2021). Strategy for stereospecific characterization of natural triacylglycerols using multidimensional chromatography and mass spectrometry. *Journal of Chromatography A*, 1641, Article 461992. <https://doi.org/10.1016/j.chroma.2021.461992>
- Kildahl-Andersen, G., Gjerlaug-Enger, E., Rise, F., Haug, A., & Egelandsdal, B. (2021). Quantification of fatty acids and their Regioisomeric distribution in Triacylglycerols from porcine and bovine sources using ¹³C NMR Spectroscopy. *Lipids*, 56(1), 111–122. <https://doi.org/10.1002/lipd.12277>
- Kozlov, O., Horáková, E., Rademacherová, S., Malinák, D., Andráš, R., Prchalová, E., & Lisa, M. (2023). Direct Chiral Supercritical Fluid Chromatography–Mass Spectrometry Analysis of Monoacylglycerol and Diacylglycerol Isomers for the Study of Lipase-Catalyzed Hydrolysis of Triacylglycerols. *Analytical Chemistry*, 95(11), 5109–5116. <https://doi.org/10.1021/acs.analchem.3c00053>
- Kruk, J., Doskocz, M., Jodłowska, E., Zacharzewska, A., Łakomic, J., Czaja, K., & Kujawski, J. (2017). NMR techniques in Metabolomic studies: A quick overview on examples of utilization. *Applied Magnetic Resonance*, 48(1), 1–21. <https://doi.org/10.1007/s00723-016-0846-9>
- Leveque, N. L., Acheampong, A., Heron, S., & Tchaplá, A. (2012). Determination of triacylglycerol regioisomers using electrospray ionization–quadrupole ion trap mass spectrometry with a kinetic method. *Analytica Chimica Acta*, 722, 80–86. <https://doi.org/10.1016/j.aca.2012.02.016>
- Li, K., Fissette, S. D., Buchinger, T. J., Middleton, Z. E., Boyer, A., & Li, W. (2018). High-performance liquid chromatography quantification of enantiomers of a Dihydroxylated tetrahydrofuran natural product. *Chirality*, 30(8), 1012–1018. <https://doi.org/10.1002/chir.22978>
- Linderborg, K. M., Kalpio, M., Makela, J., Niinikoski, H., Kallio, H. P., & Lagstrom, H. (2014). Tandem mass spectrometric analysis of human milk triacylglycerols from normal weight and overweight mothers on different diets. *Food Chemistry*, 146, 583–590. <https://doi.org/10.1016/j.foodchem.2013.09.092>
- Lisa, M., & Holcapek, M. (2013). Characterization of triacylglycerol enantiomers using chiral HPLC/APCI-MS and synthesis of enantiomeric Triacylglycerols. *Analytical Chemistry*, 85(3), 1852–1859. <https://doi.org/10.1021/ac303237a>
- Lisa, M., Velínská, H., & Holcapek, M. (2009). Regioisomeric characterization of Triacylglycerols using silver-ion HPLC/MS and randomization synthesis of standards. *Analytical Chemistry*, 81(10), 3903–3910. <https://doi.org/10.1021/ac900150j>
- Litmanovitz, I., Davidson, K., Eliakim, A., Regev, R. H., Dolfin, T., Arnon, S., ... Nemet, D. (2013). High Beta-palmitate formula and bone strength in term infants: A randomized, double-blind, controlled trial. *Calcified Tissue International*, 92(1), 35–41. <https://doi.org/10.1007/s00223-012-9664-8>
- Liu, Q., Zhao, J., Liu, Y., Qiao, W., Jiang, T., Liu, Y., Yu, X., & Chen, L. (2022). Advances in analysis, metabolism and mimicking of human milk lipids. *Food Chemistry*, 393, Article 133332. <https://doi.org/10.1016/j.foodchem.2022.133332>
- Liu, Z., & Rochfort, S. (2021). Bovine Milk triacylglycerol Regioisomer ratio shows remarkable inter-breed and inter-cow variation. *Molecules*, 26(13), 3938. <https://doi.org/10.3390/molecules26133938>
- Liu, Z., Rochfort, S., & Cocks, B. (2018). Milk lipidomics: What we know and what we don't. *Progress in Lipid Research*, 71, 70–85. <https://doi.org/10.1016/j.plipres.2018.06.002>
- Manios, Y., Karagali, E., Thijs-Verhoeven, I., Vlachopapadopoulou, E., Papazoglou, A., Maragoudaki, E., Manikas, Z., Kampani, M., Christaki, I., Vonk, M., Bos, R., & Parikh, P. (2020). Milk fat-based formula reduced palmitic acid soaps and excretion of calcium in healthy term infants: Two double-blind, randomized, cross-over trials. *Proceedings of the Nutrition Society*, 79(OCE2), E268. <https://doi.org/10.1017/S0029665120002165>
- Masuda, K., Abe, K., & Murano, Y. (2021). A practical method for analysis of triacylglycerol isomers using supercritical fluid chromatography. *Journal of the American Oil Chemists Society*, 98(1), 21–29. <https://doi.org/10.1002/aocs.12432>
- Miles, E. A., & Calder, P. C. (2017). The influence of the position of palmitate in infant formula triacylglycerols on health outcomes. *Nutrition Research*, 44, 1–8. <https://doi.org/10.1016/j.nutres.2017.05.009>
- Momchilova, S., & Nikolova-Damyanova, B. (2022). Regio- and stereospecific analysis of Triacylglycerols—A brief overview of the challenges and the achievements. *Symmetry*, 14(2), 247. <https://doi.org/10.3390/sym14020247>
- Monteiro, R. C. S., Virgen-Ortiz, J. J., Berenguer-Murcia, A., da Rocha, T. N., dos Santos, J. C. S., Alcantara, A. R., & Fernandez-Lafuente, R. (2021). Biotechnological relevance of the lipase a from *Candida antarctica*. *Catalysis Today*, 362, 141–154. <https://doi.org/10.1016/j.cattod.2020.03.026>
- Nagai, T., Kinoshita, T., Kasamatsu, E., Yoshinaga, K., Mizobe, H., Yoshida, A., ... Gotoh, N. (2019). Simultaneous separation of triacylglycerol enantiomers and positional isomers by chiral high performance liquid chromatography coupled with mass spectrometry. *Journal of Oleo Science*, 68(10), 1019–1026. <https://doi.org/10.5650/jos.ess19122>
- Nagai, T., Kinoshita, T., Kasamatsu, E., Yoshinaga, K., Mizobe, H., Yoshida, A., ... Gotoh, N. (2020). Simultaneous quantification of mixed-acid triacylglycerol positional isomers and enantiomers in palm oil and lard by chiral high-performance liquid chromatography coupled with mass spectrometry. *Symmetry*, 12(9), 1385. <https://doi.org/10.3390/sym12091385>
- Nagai, T., Matsumoto, Y., Jiang, Y., Ishikawa, K., Wakatabe, T., Mizobe, H., ... Gotoh, N. (2013). Actual ratios of triacylglycerol positional isomers and enantiomers comprising saturated fatty acids and highly unsaturated fatty acids in fishes and marine mammals. *Journal of Oleo Science*, 62(12), 1009–1015. <https://doi.org/10.5650/jos.62.1009>
- Nagai, T., Mizobe, H., Otake, I., Ichioka, K., Kojima, K., Matsumoto, Y., Gotoh, N., Kuroda, I., & Wada, S. (2011). Enantiomeric separation of asymmetric triacylglycerol by recycle high-performance liquid chromatography with chiral column. *Journal of Chromatography A*, 1218(20), 2880–2886. <https://doi.org/10.1016/j.chroma.2011.02.067>
- Nagar, T., Ishikawa, K., Yoshinaga, K., Yoshida, A., Beppu, F., & Gotoh, N. (2017). Homochiral asymmetric triacylglycerol isomers in egg yolk. *Journal of Oleo Science*, 66(12), 1293–1299. <https://doi.org/10.5650/jos.ess17128>
- Pchelkin, V. P., Kuznetsova, E. I., Tsyndambaev, V. D., & Vereshchagin, A. G. (2001). Determination of the positional-species composition of plant reserve triacylglycerols by partial chemical deacylation. *Russian Journal of Plant Physiology*, 48(5), 701–707. <https://doi.org/10.1023/A:1016732708350>
- Qi, C., Sun, J., Xia, Y., Yu, R., Wei, W., Xiang, J., ... Wang, X. (2018). Fatty acid profile and the sn-2 position distribution in Triacylglycerols of breast Milk during different lactation stages. *Journal of Agricultural and Food Chemistry*, 66(12), 3118–3126. <https://doi.org/10.1021/acs.jafc.8b01085>
- Roman, C., Carriere, F., Villeneuve, P., Pina, M., Millet, V., Simeoni, U., & Sarles, J. (2007). Quantitative and qualitative study of gastric lipolysis in premature infants: Do MCT-enriched infant formulas improve fat digestion? *Pediatric Research*, 61(1), 83–88. <https://doi.org/10.1203/01.pdr.0000250199.24107.fb>
- Salas, J. J., Bootello, M. A., Martínez-Force, E., & Garcés, R. (2011). Production of stearate-rich butters by solvent fractionation of high stearic–high oleic sunflower oil. *Food Chemistry*, 124(2), 450–458. <https://doi.org/10.1016/j.foodchem.2010.06.053>
- Santoro, V., Dal Bello, F., Aigotti, R., Gastaldi, D., Romaniello, F., Forte, E., ... Medana, C. (2018). Characterization and determination of Interesterification markers

- (triacylglycerol Regioisomers) in confectionery oils by liquid chromatography-mass spectrometry. *Foods*, 7(2), 23. <https://doi.org/10.3390/foods7020023>
- Sazzad, M. A. A., Fabritius, M., Bostrom, P., Tarvainen, M., Kalpio, M., Linderborg, K. M., ... Yang, B. (2022). A novel UHPLC-ESI-MS/MS method and automatic calculation software for regiospecific analysis of triacylglycerols in natural fats and oils. *Analytica Chimica Acta*, 1210, Article 339887. <https://doi.org/10.1016/j.aca.2022.339887>
- Sun, C., Wei, W., Su, H., Zou, X., & Wang, X. (2018). Evaluation of sn-2 fatty acid composition in commercial infant formulas on the Chinese market: A comparative study based on fat source and stage. *Food Chemistry*, 242, 29–36. <https://doi.org/10.1016/j.foodchem.2017.09.005>
- Takeda, H., Izumi, Y., Takahashi, M., Paxton, T., Tamura, S., Koike, T., Yu, Y., Kato, N., Nagase, K., Shiomi, M., & Bamba, T. (2018). Widely-targeted quantitative lipidomics method by supercritical fluid chromatography triple quadrupole mass spectrometry. *Journal of Lipid Research*, 59(7), 1283–1293. <https://doi.org/10.1194/jlr.D083014>
- Tarvainen, M., Kallio, H., & Yang, B. (2019). Regiospecific analysis of Triacylglycerols by ultrahigh-performance-liquid chromatography-electrospray ionization-tandem mass spectrometry. *Analytical Chemistry*, 91(21), 13695–13702. <https://doi.org/10.1021/acs.analchem.9b02968>
- Tyskiewicz, K., Debczak, A., Gieysztor, R., Szymczak, T., & Roj, E. (2018). Determination of fat-and water-soluble vitamins by supercritical fluid chromatography: A review. *Journal of Separation Science*, 41(1), 336–350. <https://doi.org/10.1002/jssc.201700598>
- Wang, S., Zheng, C., Guo, D., Chen, W., Xie, Q., & Zhai, Q. (2023). Dose-related effects of sn-2 palmitate, a specific positional distributed human milk fatty acid, intake in early life on the composition and metabolism of the intestinal microbiota. *Journal of Dairy Science*. <https://doi.org/10.3168/jds.2023-23361>
- Wei, W., Sun, C., Wang, X., Jin, Q., Xu, X., Akoh, C. C., & Wang, X. (2020). Lipase-catalyzed synthesis of Sn-2 palmitate: A review. *Engineering*, 6(4), 406–414. <https://doi.org/10.1016/j.eng.2020.02.008>
- Wu, W., Zhao, A., Liu, B., Ye, W.-H., Su, H.-W., Li, J., & Zhang, Y.-M. (2021). Neurodevelopmental outcomes and gut Bifidobacteria in term infants fed an infant formula containing high sn-2 palmitate: A cluster randomized clinical trial. *Nutrients*, 13(2), 693. <https://doi.org/10.3390/nu13020693>
- Xia, T., Yuan, M., Xu, Y., Zhou, F., Yu, K., & Xia, Y. (2021). Deep structural annotation of Glycerolipids by the charge-tagging Paterno-Buchi reaction and supercritical fluid chromatography-ion mobility mass spectrometry. *Analytical Chemistry*, 93(23), 8345–8353. <https://doi.org/10.1021/acs.analchem.1c01379>
- Yang, B., & Kallio, H. (2006). Analysis of triacylglycerols of seeds and berries of sea buckthorn (*Hippophae rhamnoides*) of different origins by mass spectrometry and tandem mass spectrometry. *Lipids*, 41(4), 381–392. <https://doi.org/10.1007/s11745-006-5109-3>
- Yang, W., Zhang, Y., Pan, H., Yao, C., Hou, J., Yao, S., Cai, L., Feng, R., Wu, W., & Guo, D. (2017). Supercritical fluid chromatography for separation and preparation of tautomeric 7-epimeric spiro oxindole alkaloids from *Uncaria macrophylla*. *Journal of Pharmaceutical and Biomedical Analysis*, 134, 352–360. <https://doi.org/10.1016/j.jpba.2016.10.021>
- Yang, Y., Liang, Y., Yang, J., Ye, F., Zhou, T., & Li, G. (2019). Advances of supercritical fluid chromatography in lipid profiling. *Journal of Pharmaceutical Analysis*, 9(1), 1–8. <https://doi.org/10.1016/j.jpha.2018.11.003>
- Yoshinaga, K. (2021). Development of analytical methods and nutritional studies using synthetic fatty acids and Triacylglycerols. *Journal of Oleo Science*, 70(1), 1–9. <https://doi.org/10.5650/jos.ess20196>
- Yu, J., Yan, Z., Mi, L., Wang, L., Liu, Z., Ye, X., ... Wang, X. (2022). Medium- and long-chain triacylglycerols and di-unsaturated fatty acyl-palmitoyl-glycerols in Chinese human milk: Association with region during the lactation. *Frontiers in Nutrition*, 9, 1040321. <https://doi.org/10.3389/fnut.2022.1040321>
- Yuan, T., Geng, Z., Dai, X., Zhang, X., Wei, W., Wang, X., & Jin, Q. (2020). Triacylglycerol containing medium-chain fatty acids: Comparison of human Milk and infant formulas on lipolysis during in vitro digestion. *Journal of Agricultural and Food Chemistry*, 68(14), 4187–4195. <https://doi.org/10.1021/acs.jafc.9b07481>
- Zhang, C., Xu, X., Zhang, S., Xiao, M., Liu, Y., Li, J., Du, G., Lv, X., Chen, J., & Liu, L. (2024). Detection and analysis of triacylglycerol regioisomers via electron activated dissociation (EAD) tandem mass spectrometry. *Talanta*, 270, Article 125552. <https://doi.org/10.1016/j.talanta.2023.125552>
- Zhang, X., Wei, W., Tao, G., Jin, Q., & Wang, X. (2021). Identification and quantification of Triacylglycerols using Ultraperformance supercritical fluid chromatography and quadrupole time-of-flight mass spectrometry: Comparison of human Milk, infant formula, other mammalian Milk, and plant oil. *Journal of Agricultural and Food Chemistry*, 69(32), 8991–9003. <https://doi.org/10.1021/acs.jafc.0c07312>
- Zhang, X., Wei, W., Tao, G., Jin, Q., & Wang, X. (2022). Triacylglycerol regioisomers containing palmitic acid analyzed by ultra-performance supercritical fluid chromatography and quadrupole time-of-flight mass spectrometry: Comparison of standard curve calibration and calculation equation. *Food Chemistry*, 391, Article 133280. <https://doi.org/10.1016/j.foodchem.2022.133280>
- Zhao, J., Liu, Q., Liu, Y., Qiao, W., Yang, K., Jiang, T., Hou, J., Zhou, H., Zhao, Y., Lin, T., Li, N., & Chen, L. (2021). Quantitative profiling of glycerides, glycerophosphatides and sphingolipids in Chinese human milk with ultra-performance liquid chromatography/quadrupole-time-of-flight mass spectrometry. *Food Chemistry*, 346, Article 128857. <https://doi.org/10.1016/j.foodchem.2020.128857>
- Zhu, L., Fang, S., Liu, W., Zhang, H., Zhang, Y., Xie, Z., Yang, P., Wan, J., Gao, B., & Yu, L. (2023). The triacylglycerol structure and composition of a human milk fat substitute affect the absorption of fatty acids and calcium, lipid metabolism and bile acid metabolism in newly-weaned Sprague-Dawley rats. *Food & Function*, 14(16), 7574–7585. <https://doi.org/10.1039/d2fo01800d>